Deep structures of the Palawan and Sulu Sea and their implications for opening of the South China Sea

Article *in* Marine and Petroleum Geology · December 2014

DOI: 10.1016/j.marpetgeo.2014.06.005

CITATIONS
7

READS
398

5 authors, including:

Chun-Feng Li
Zhejiang University
51 PUBLICATIONS **585** CITATIONS
SEE PROFILE

J. Li
1,518 PUBLICATIONS **16,152** CITATIONS
SEE PROFILE

Zuyi Zhou
Tongji University
25 PUBLICATIONS **548** CITATIONS
SEE PROFILE

Marine and Petroleum Geology 58 (2014) 721–735

Contents lists available at ScienceDirect

Marine and Petroleum Geology

journal homepage: www.elsevier.com/locate/marpetgeo

Research paper

Deep structures of the Palawan and Sulu Sea and their implications for opening of the South China Sea

Wei-Nan Liu [a], Chun-Feng Li [a, *], Jiabiao Li [b], Derek Fairhead [c], Zuyi Zhou [a]

[a] State Key Laboratory of Marine Geology, Tongji University, Shanghai 200092, PR China
[b] 2nd Institute of Oceanography, State Oceanic Administration, Hangzhou 310012, Zhejiang, PR China
[c] Getech, Kitson House, Elmete Hall, Elmete Lane, Leeds LS8 2LJ, United Kingdom

ARTICLE INFO

Article history:
Received 23 June 2013
Received in revised form
22 April 2014
Accepted 6 June 2014
Available online 19 June 2014

Keywords:
Sulu Sea
Palawan Continental Block
South China Sea
Relict oceanic crust
Curie depth
Moho

ABSTRACT

Compared to the northern South China Sea continental margin, the deep structures and tectonic evolution of the Palawan and Sulu Sea and ambient regions are not well understood so far. However, this part of the southern continental margin and adjacent areas embed critical information on the opening of the South China Sea (SCS). In this paper, we carry out geophysical investigations using regional magnetic, gravity and reflection seismic data. Analytical signal amplitudes (ASA) of magnetic anomalies are calculated to depict the boundaries of different tectonic units. Curie-point depths are estimated from magnetic anomalies using a windowed wavenumber-domain algorithm. Application of the Parker–Oldenburg algorithm to Bouguer gravity anomalies yields a 3D Moho topography. The Palawan Continental Block (PCB) is defined by quiet magnetic anomalies, low ASA, moderate depths to the top and bottom of the magnetic layer, and its northern boundary is further constrained by reflection seismic data and Moho interpretation. The PCB is found to be a favorable area for hydrocarbon exploration. However, the continent–ocean transition zone between the PCB and the SCS is characterized by hyper-extended continental crust intruded with magmatic bodies. The NW Sulu Sea is interpreted as a relict oceanic slice and the geometry and position of extinct trench of the Proto South China Sea (PSCS) is further constrained. With additional age constraints from inverted Moho and Curie-point depths, we confirm that the spreading of the SE Sulu Sea started in the Early Oligocene/Late Eocene due to the subduction of the PSCS, and terminated in the Middle Miocene by the obduction of the NW Sulu Sea onto the PCB.

1. Introduction

To better understand the opening processes of the South China Sea (SCS), an Atlantic-type marginal sea from continental rifting (e.g., Taylor and Hayes, 1980, 1983), it is critical to compare tectonics and deep structures of its two conjugate continental margins. The southern margin experienced a long history of Mesozoic paleo-Pacific subduction (Li and Li, 2007; Li et al., 2012), and Cenozoic subduction of the proto-South China Sea (PSCS) and its interactions with the Sulu Sea to the south. Different types of terrains (oceanic crust, continent–ocean transition zone, continental block, island arc) amalgamated here but their boundaries are not well defined and the origin of some tectonic units along the southern margin remains uncertain (e.g., Franke et al., 2008, 2011), because of complicated rifting and collision processes that have occurred.

The tectonic models for the southern margin involve two main types: collision–extrusion model (Briais et al., 1993; Replumaz and Tapponnier, 2003) and subduction–collision model (Hamilton, 1979; Lee and Lawver, 1995; Hall, 1996). The main differences of the two models are in the aspects of the mechanism responsible for rifting and seafloor spreading in the South China Sea, the amount of displacement along the Red River fault and the size of a pre-existing ocean basin (the proto South China Sea, PSCS) subducted beneath Borneo.

The southern South China Sea continental margin today is also in direct contact with the Sulu Sea, the tectonic evolution of which is still not well understood. Although ODP Leg 124 was implemented in the Sulu and Celebes Seas in 1990, many key issues are still unsolved (Rangin and Silver, 1991; Silver and Rangin, 1991). The origin of the NW Sulu Sea is rarely discussed in previous studies, and different hypothetic models are presented for the evolution of the SE Sulu Sea, either as a back-arc basin triggered by the subduction of the PSCS (Rangin and Silver, 1991) or the Celebes Sea plate (Rangin, 1989), or a marginal basin analogous to the SCS

* Corresponding author.
E-mail address: cfl@tongji.edu.cn (C.-F. Li).

http://dx.doi.org/10.1016/j.marpetgeo.2014.06.005
0264-8172/

(Rangin and Silver, 1991). Moreover, the formation timing of the SE Sulu Sea, either the Early Miocene (Rangin and Silver, 1991) or the Oligocene (Roeser, 1991), is also in debate. Drilled at a location quite near to an arc (Cagayan Ridge), Site 769 of ODP Leg 124 (Fig. 2) did not sample the oldest oceanic basement of the Sulu Sea. Magnetic anomalies in the SE Sulu Sea are not parallel to the Cagayan Ridge (Fig. 3), and the oldest anomalies cannot be well recognized and have been largely subducted beneath the Negros Trench and Sulu Trench.

This paper explores topography, gravity, magnetic, and seismic data to better understand the tectonic complexity, deep structures, and hydrocarbon potential of the Palawan and Sulu Sea area and their surroundings. We have carried out various data processing and geophysical inversions, including analytic signal analysis and inversion of Curie depth and Moho depth.

2. Tectonic framework

The Palawan Continental Block (PCB) and Sulu Sea are surrounded by the SCS, Philippine Archipelago, Celebes Sea and Borneo (Figs. 1 and 2). The main Palawan Island is NE–SW trending and is made up of two parts, namely, the north Palawan formed by continent-originated sedimentary and metamorphic blocks drifted from the Eurasian continental margin with the opening of the SCS between ~32 Ma and ~16 Ma (Holloway, 1982; Taylor and Hayes, 1980, 1983; Sales et al., 1997; Almasco et al., 2000; Suzuki et al., 2000a, 2000b; Aurelio et al., 2012; Shi and Li, 2012), and the Early Cretaceous to Eocene oceanic rock formations (the Palawan Ophiolite Complex) exposed in the south Palawan (Raschka et al., 1985; Letouzey et al., 1988; Faure et al., 1989; Müller, 1991; Fuller et al., 1991; Encarnación, 2004). The Palawan Ophiolite Complex is equivalent in origin to the ophiolites of Borneo (Rangin et al., 1990; Schlüter et al., 1996; Cullen, 2010). The boundary between the north and south Palawan is partly defined by the Ulugan Bay fault (Figs. 1 and 2) (Yumul et al., 2009). Northeast of Palawan is a group of small islands that belong to the Calamian Island Group. The PCB contains the Reed Bank and the north Palawan. Borneo is located to the southwest of the Palawan Island, and Sabah sits on the northern portion of Borneo.

A linear trough called the Palawan Trough lies in the SCS southern coastal zone, and it connects with the Borneo Trough to the south. The Palawan and Borneo Troughs were interpreted as the extinct trench of the southern convergent margin of the Proto South China Sea (PSCS) (Hamilton, 1979; Hinz et al., 1989; Lee and Lawver, 1995; Hall, 1996, 2011; Morley, 2002; Hall et al., 2008), but the existence of the trench between the Reed Bank and the Calamian Island Group cannot be reconciled with the north Palawan continental strata as old as Permian that drifted southeastward from Eurasia (Taylor and Hayes, 1980, 1983; Fontaine, 1979; Mitchell and Leach, 1991; Almasco et al., 2000; Suzuki et al., 2000b; Li et al., 2007; Shi and Li, 2012). Therefore, it can be confirmed that the Palawan Trough was not associated with the

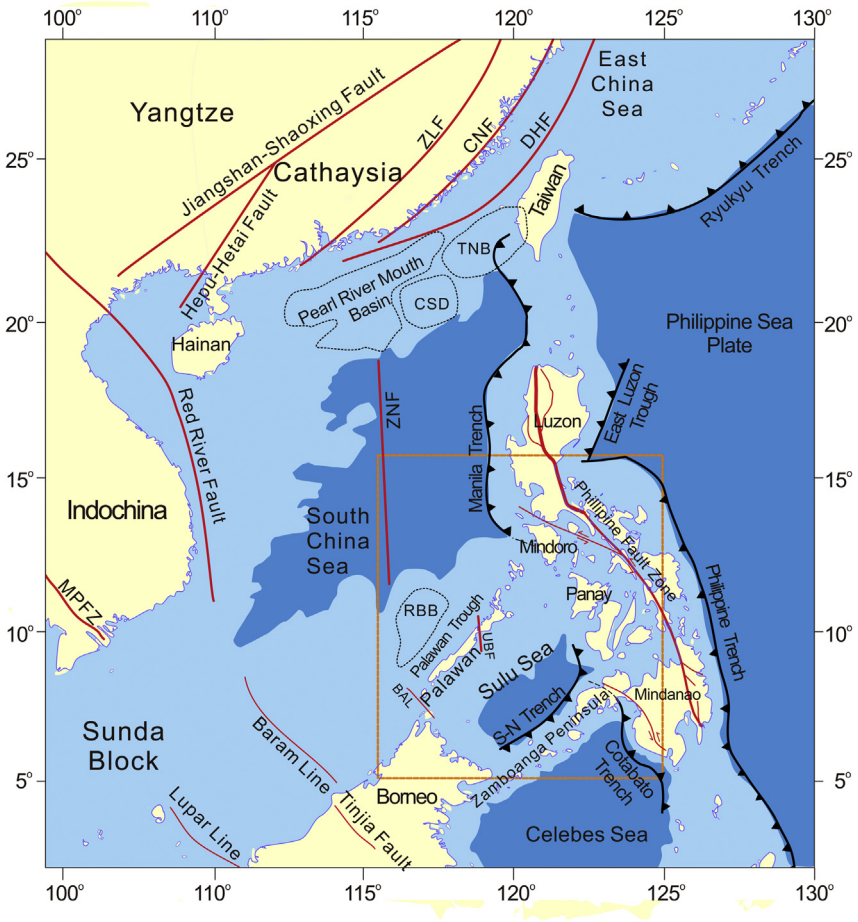

Figure 1. Regional tectonic and geological features of SE Asia. Major tectonic elements: ZLF = Zhenghe-Lianhuashan Fault, CNF = Changle-Nan'ao Fault, CR=Cagayan Ridge, DHF = Donghai Fault, ZNF = Zhongnan Fault, MPFZ = Mae Ping Fault Zone, BAL=Balabac Line, UBF=Ulugan Bay Fault, TNB = Tainan Basin, CSD=Chaoshan Depression, RBB = Reed Bank Basin. The box is the study area of this paper and details are shown in Fig. 2.

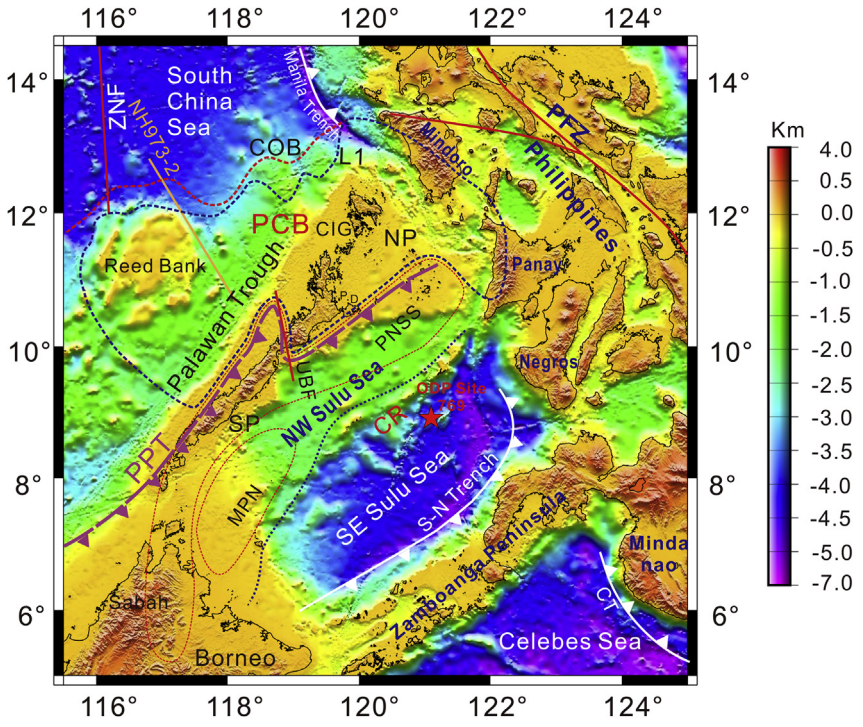

Figure 2. Regional topographic map showing major tectonic units. Notes: ZNF = Zhongnan Fault, CIG = Calamian Island Group, PCB = Palawan Continental Block, NP = North Palawan, SP = South Palawan, UBF = Ulugan Bay Fault, BAL = Balabac Line, P = Paly Island, D = Dumaran Island, CR = Cagayan Ridge, S-N Trench = Sulu-Negros Trench, CT = Cotabato Trench, PFZ = Philippine Fault Zone. PPT = Proto Palawan Trench. Line NH973-2 is the multichannel reflection seismic shown in Fig. 5. L1 = the boundary of PCB defined by magnetic anomalies and ASA. COB = the continent–ocean boundary constrained by gravity anomalies and seismic data. Black contours are coastal lines. The red star represents the location of site 769 of ODP Leg 124 in the Sulu Sea. (For interpretation of the references to color in this figure legend, the reader is referred to the web version of this article.)

ancient subduction zone of the PSCS (Hinz and Schlüter, 1985; Milsom et al., 1997; Ingram et al., 2004; Hesse et al., 2009).

The NE–SW trending Cagayan Ridge divides the Sulu Sea into two subbasins of quite different bathymetric features, the NW Sulu Sea and the SE Sulu Sea. The abyssal plain of the SE Sulu Basin is situated between the Cagayan Ridge and Zamboanga Peninsula (Fig. 2) (Schlüter et al., 1996). The SE Sulu Sea plate is subducting beneath the Negros and Zamboanga Peninsula along the Sulu-Negros Trench (Pubellier et al., 1991; Castillo et al., 2007). The Sulu Arc is a NE-trending linear chain of small volcanic islands along the boundary between the Sulu and Celebes Sea (Castillo et al., 2007).

3. The boundary of the Palawan Continental Block (PCB)

The PCB is not a unified single block from the topographic map (Fig. 2). However, its geophysical properties are remarkably uniform, suggesting a common geological origin. Here we characterize the boundary of this block using geophysical data.

3.1. Analytic signal analysis of magnetic anomalies

The total field magnetic anomaly data (Fig. 3) used in this study are from two sources. One is compiled by Geological Survey of Japan and Coordinating Committee for Coastal and Offshore Geoscience Programmes in East and Southeast Asia(CCOP, 1996), and the other set is the magnetic data for the Philippines from an aeromagnetic survey in 1982 with a 2 km line spacing in mainly NE–SW line direction. The latter set is well complementary to the first one, and fills data gaps in the Philippines. We merge these two sets of data together and space them based on 1-min gridding.

3D analytical signal amplitudes (ASA) (Fig. 4) are calculated from the total field magnetic anomaly data. ASA is defined as

$$|A(x,y)| = \sqrt{(\partial M/\partial x)^2 + (\partial M/\partial y)^2 + (\partial M/\partial z)^2}, \quad (1)$$

where $|A(x,y)|$ is analytic signal amplitude at (x,y), and M is the observed magnetic field at (x,y) (Nabighian, 1984; Ofoegbu and Mohan, 1990; Roest et al., 1992). ASA is essentially equivalent to the total magnetic gradient and is independent of the inclination and declination of the source magnetization and the Earth's magnetic field if the magnetic contacts are nearly vertical (Nabighian, 1972; Agarwal and Shaw, 1996; Salem et al., 2002; Li, 2006). Analytic signal analysis can be, to some extent, complementary and/or equivalent to reduction to the pole (Li, 2006; Li et al., 2008), and the latter procedure has great difficulties and limitations in low latitude areas (MacLeod et al., 1994; Blakely, 1996). ASA makes the geological interpretation more straightforward since ASA is always positive, with peak tending to be located directly above the magnetic sources and/or the contacts (MacLeod et al., 1994; Li, 2006; Li et al., 2008). Analytic signal analysis reduces magnetic data to anomalies whose maxima mark the edges or centers of magnetized bodies, and whose shape can be used to determine the depths of magnetic sources. The effectiveness of ASA has been demonstrated in mapping magmatic sources in the South China Sea and east China (Li et al., 2008; Zhang and Li, 2011).

From the ASA map (Fig. 4), sharper contrasts between different tectonic units are observed than from the total field magnetic anomalies (Fig. 3). The ASA shows an obvious boundary corresponding to the Ulugan Bay fault between the north and south Palawan. A high ASA zone covers the south Palawan and extends into the NW Sulu Sea and NE Sabah (Fig. 4), an observation conformable

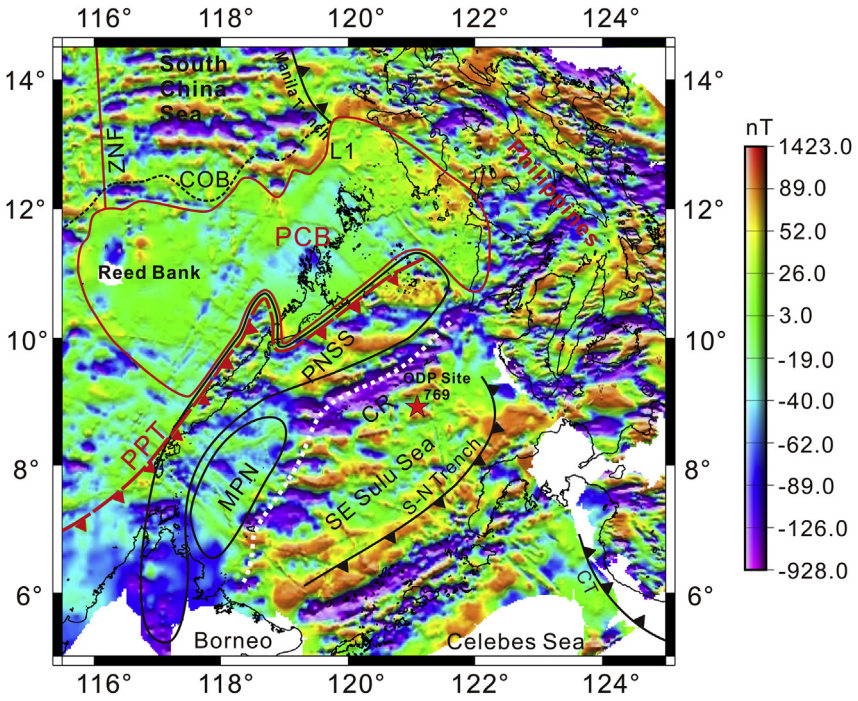

Figure 3. Total field magnetic anomaly map of the Palawan-Sulu Sea area. PPT = Proto Palawan Trench. PNSS = Proto NW Sulu Sea, MPN = Margin of Proto NW Sulu Sea (see the explanation in the Discussion). See Fig. 2 for other notations.

to the interpretation that the south Palawan comprises an oceanic crust originated from farther south (Almasco et al., 2000). A magnetically quiet zone, conspicuously located to the south of SCS and west of Philippine Mobile Belt, corresponds to the PCB. This magnetically quiet zone has a counterpart in the northern SCS margin, the area covering the Tainan Basin and Chaoshan Depression where there are thick Mesozoic and Cenozoic sedimentary rocks with weak magnetic susceptibilities (Li and Song, 2012; Shi and Li, 2012). Linear zones of high ASA along the volcanic Cagayan Ridge and Sulu Arc are observed from the ASA map (Fig. 4).

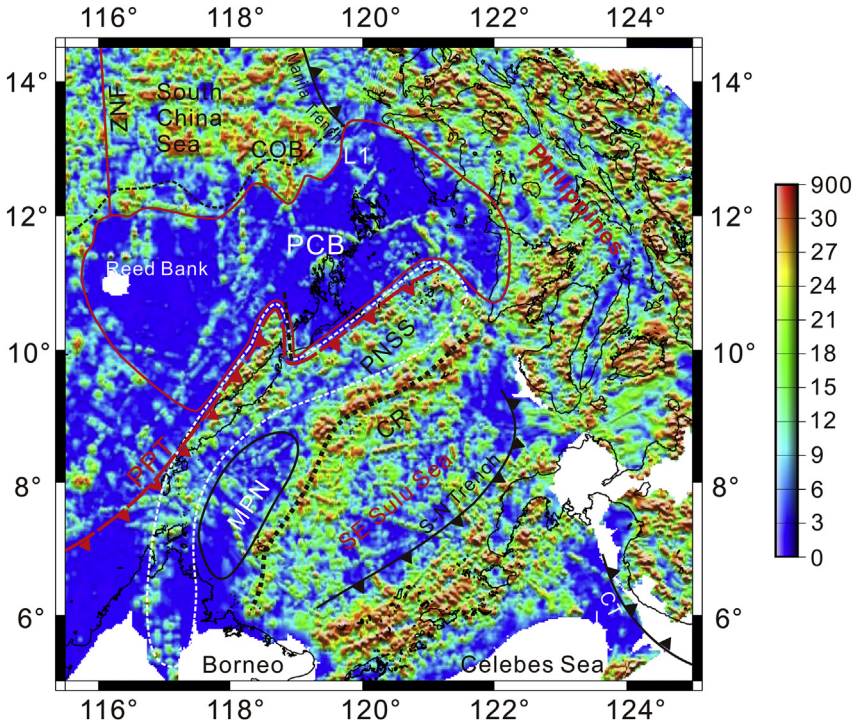

Figure 4. Regional Map of analytical signal amplitudes calculated from regional total field magnetic anomalies. Black dotted line represents the Ulugan Bay fault. See Figures 2 and 3 for other notations.

3.2. The continent–ocean boundary between the SCS and PCB

The northern limit of the PCB identified from ASA may not coincide with the continent–ocean boundary (COB) between the SCS and PCB, because a wide variety of rocks types could be exposed proximal to the COB due to rather complicated nonuniform depth-dependent extension during the continental breakup (e.g., Huismans and Beaumont, 2011). Volcanism and mafic/ultramafic rock exposure along the COB can all contribute to high ASA. Collectively, stronger magnetic (and ASA) anomalies from the oceanic crust and higher Bouguer gravity anomalies originated from elevated Moho often signify the location of the COB. In addition, deep penetrating reflection seismic data can provide fine-scale constraints on the attitude of the COB (Fig. 4).

A recently acquired seismic reflection line NH973-2 near the Reed Bank further pinpoints the northern extent of the PCB (Fig. 5). This line was acquired in 2009 with the Chinese R/V "Tanbao", using a 6237.5 m long streamer with 480 channels. The data were recorded up to 12 s at a 2 ms sampling interval. Pre-stack processing of these seismic data includes amplitude compensation, static correction, gain and mute analysis, predictive deconvolution, multiple attenuation, velocity analysis, residual static corrections and frequency filtering. Post-stack deconvolution, band-pass and coherency filtering are then applied to the stacked data, before a finite-difference migration.

As interpreted by Ding and Li (2011), three distinct tectono-stratigraphic areas are imaged from southeast to northwest, namely the graben basin (between the Reed Bank and the Palawan), the Reed Bank, and the oceanic basin of the South China Sea (Fig. 5). The graben basin in the Palawan Trough is characterized by a series of seaward dipping normal faults that control half grabens. This deformation style is almost identical to development of faults and half grabens in the northern SCS continental margin, suggesting for an early simple shear rifting model. These faults were mainly active in early rifting and drifting stage of the SCS (Ding and Li, 2011). Like the Chaoshan block in the northern SCS continental margin, which was surrounded by a rifting belt but remained stable inside during the rifting phase (Shi and Li, 2012), the Reed Bank recorded little deformation and remained largely intact during early rifting. The area to the north of the Reed Bank shows very thin crust on the seismic section, and the Moho reflector can be recognized at ~8.3 s in two-way travel time (Fig. 5).

From the seismic section and gravity anomalies, we confirm that the COB is located further north to the northern boundary of the

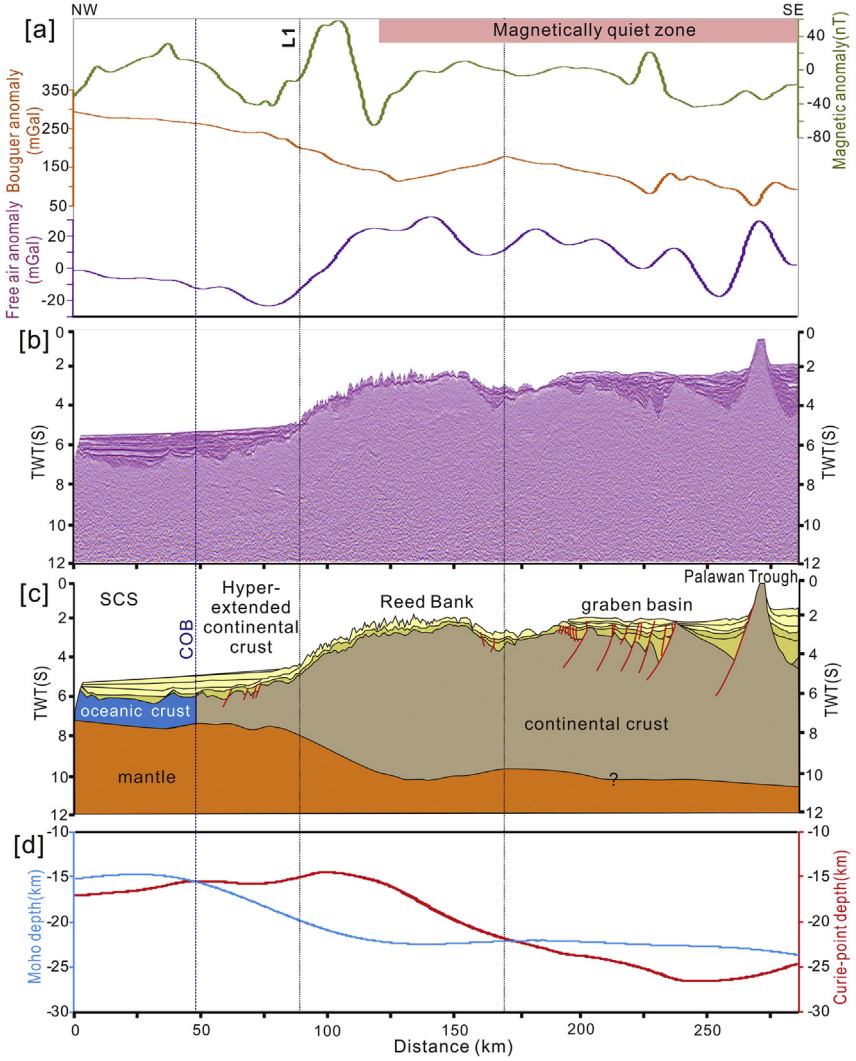

Figure 5. Geophysical profile along the multichannel reflection seismic line NH973-2 revealing the relationships between key tectonic boundaries. [a] Gravity and magnetic anomalies. [b] Seismic profile. [c] Geological interpretation of the seismic profile. [d] Estimated Moho and Curie depths along the profile. COB = continental-ocean boundary.

PCB identified from magnetic anomalies (marked as L1 in figures). The COB marks the seaward limit of a low free-air gravity anomaly belt (Fig. 5). Sharp changes in seismic facies are also observed across the COB, although the crustal thickness remains almost the same. We interpret that the low free-air gravity anomaly belt is caused by extremely thinned continental lithosphere to the landward side of the COB. Faulted blocks and chaotic reflections there support this reasoning. The large ASA and strong magnetic anomalies within the zone of hyper-extended continental lithosphere suggest that strong magmatism occurred in the zone between the COB and L1 (Figs. 3 and 4), as previously suggested by Franke et al. (2011). However, we cannot constrain the timing of the magmatism at this moment.

4. Depths to magnetic sources

4.1. Curie-point depths

Very few valid heat flow data are published in the Palawan and Sulu Sea region so far (Nagao and Uyeda, 1995), and the deep geothermal structure of this region has rarely been discussed. Geothermal evolution needs to be better understood to help evaluate hydrocarbon potentials and regional tectonic events.

Surface magnetic anomalies have a close connection with the Earth's geothermal field, because the magnetization of rock can be strongly affected by temperature variation. The bottom of the magnetic layer constitutes an undulating surface in the Earth's interior, below which minerals reach their Curie temperatures (about 550 °C but slightly variable with composition) and lose their ferromagnetism. Inversion of magnetic data has become a prevalent technique in depicting the geothermal structure (Okubo et al., 1985; Agrawal et al., 1992; Blakely, 1996; Tanaka et al., 1999; Ross et al., 2006; Ravat et al., 2007; Li et al., 2009, 2010). Our estimation of Curie-point depths in the Palawan and Sulu Sea region is based on radially averaged amplitude spectra of total field magnetic anomalies (e.g., Tanaka et al., 1999; Li, 2005; Li et al., 2010).

For a model with 2D horizontal fractal magnetization but a constant vertical magnetization, the 1D radial amplitude spectrum can be written as (Blakely, 1996; Li et al., 2009, 2010, 2013)

$$\ln\left[A_{\Delta T}(k,Z_t,Z_b,\beta^p_{3D})\right] = C - |2\pi k|Z_t - \frac{\beta^p_{3D}-1}{2}\ln|2\pi k| + \ln\left[1-e^{-|2\pi k|(Z_b-Z_t)}\right], \quad (2)$$

with the assumptions of infinite horizontal extensions of magnetic sources and much smaller depths than horizontal scales. Here $A_{\Delta T}$ is the radially averaged amplitude spectrum of the total field magnetic anomalies, C is a constant related to magnetization direction and geomagnetic field direction, wavenumber $k=\sqrt{k_x^2+k_y^2}$, and Z_b and Z_t are depths to the bottom and top of the magnetic layer, respectively. Note here that the fractal exponent β^p_{3D} is defined in the power spectrum of the 3D magnetization, and it has been shown that β^p_{3D} is nearly larger by 1 than that of a model with a 2D horizontal fractal magnetization but a constant vertical magnetization (Maus and Dimri, 1994; Maus et al., 1997; Bouligand et al., 2009). Thus, $\beta^p_{3D}-1\approx\beta^p_{2D}$.

It can be further shown mathematically that, for sufficiently large k, the last term in Eq. (2) will asymptotically become zero. Therefore,

$$\ln\left[A_{\Delta T}(k,Z_t,\beta^p_{3D})\right] \approx C1 - |2\pi k|Z_t - \frac{\beta^p_{3D}-1}{2}\ln|2\pi k|, \quad (3)$$

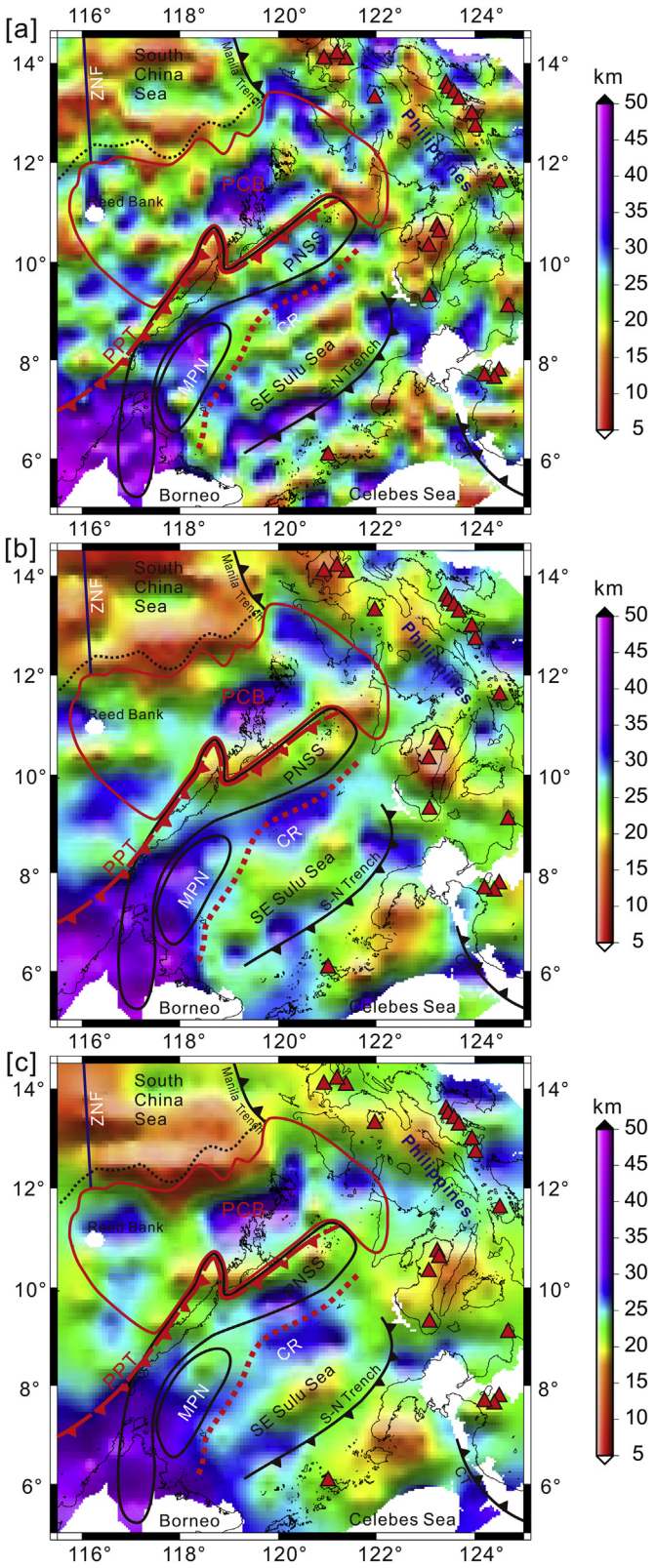

Figure 6. Maps of Curie-point depths calculated from using window sizes in 60 km × 60 km[a], 100 km × 100 km[b] and 150 km × 150 km[c]. Red triangles represent the active volcanoes in the recent 2000 years. See Figures 2 and 3 for other notations. (For interpretation of the references to color in this figure legend, the reader is referred to the web version of this article.)

where C1 is a constant. Eq. (3) forms the linearized basis of estimating Z_t at intermediate to high wavenumber band. At small wavenumber band, Tanaka et al. (1999) approximated Eq. (2) by a linear formula of the depth to the centroid Z_0 of the magnetic layer:

$$\ln\left[\frac{A_{\Delta T}(k, Z_0, \beta^p_{3D})}{|2\pi k|}\right] \approx C2 - |2\pi k| Z_0 - \frac{\beta^p_{3D} - 1}{2}\ln|2\pi k|. \quad (4)$$

The centroid is the mid-point between the top and bottom of the magnetic source.

The fractal exponent β^p_{3D} normally needs to be pre-assigned to reduce the number of unknowns to be inverted and to keep the algorithm stable. In a previous study in the SCS, Li et al. (2010) assumed that $\beta^p_{3D} = 1$ (or equivalently $\beta^p_{2D} = 0$), meaning no correlations in the 2D horizontal magnetization. However, geological features and their physical properties are normally correlated in the map view. Correction for β^p_{3D} is to consider the correlation effects in naturally distributed magnetic sources, and allows more accurate depth estimation (Li et al., 2013). The estimated Curie depths tend to be smaller with larger β^p_{3D}, but the overall areal pattern of estimated Curie depth will not change largely. Since considering a β^p_{3D} larger than 1 is theoretically more sound, we tested different β^p_{3D} and found that a β^p_{3D} of 2.5 for the study area gives the optimal results that fit known geological information, e.g., known basement depths in SCS and volcano distributions in the Philippines (Fig. 6).

Corrections for β^p_{3D} amounts to add the last term, $((\beta^p_{3D} - 1)/2)\ln|2\pi k|$, in Eqs. (3) and (4) to the spectra. After this correction, we can easily estimate Z_t and Z_0 from simple linear regressions at intermediate to high wavenumber band and small wavenumber band, respectively. The Curie depth $Z_b = 2Z_0 - Z_t$.

Figure 6 shows calculated Curie-point depths using three different window sizes in 150 km × 150 km, 100 km × 100 km, and 60 km × 60 km, respectively. The resolution of the results depends on the window size. We can constrain finer thermal structures of different tectonic units in smaller window size (Fig. 6a). But small windows may not be able to capture long wavelength components caused by very deep magnetic sources, resulting in underestimated Curie point depths. Conversely, large windows can avoid this potential problem but the results will be in low resolution. Nevertheless, the overall patterns remain the same regardless of the sizes of windows selected. Therefore, Curie depths from different windows are complementary to one another. A better solution is to simply calculate the average Curie depths from those estimated using many different windows (Fig. 7). Such a strategy can suppress local errors inherited in using a particular window (Li and Song, 2012).

From all these maps, the PCB shows variable but intermediate Curie depths. The transitional zone of hyper-extended continental crust (zone between COB and L1 in Fig. 7) shows much smaller Curie depths, similar to those of the central SCS basin. The Reed Bank and north Palawan have large Curie depths, and the largest Curie depth appears in the Borneo. Relatively shallower bottoms of magnetic layer are located in the SCS basin and Sulu Arc. The areas with small curie depths in central Philippines, Negros and Zamboanga Peninsula have good accordance with the locations of active volcanoes erupted in the past 2000 years. The deviation between the positions of some active volcanoes and shallow Curie depths may be attributed either to low resolution resulting from the limit of the window size, or to deep magma sources being not directly beneath the volcanic craters. Our results also confirm high geothermal gradient in southeastern portions of Sulu Sea near the Sulu-Negros Trench, resulting possibly from the subduction of the extinct SE Sulu spreading center (Hinz and Block, 1990; Sajona et al., 1996). With deeper Curie-point depths, the SE Sulu Sea crust appears to be much cooler compared with that of the SCS (Figs. 6 and 7). This implies that the SE Sulu Sea should be older than the SCS based on the geothermal field.

4.2. Depths to the top of magnetic sources

Similar to inverted Curie depths, higher resolution in depths to the top of magnetic sources have been shown using smaller

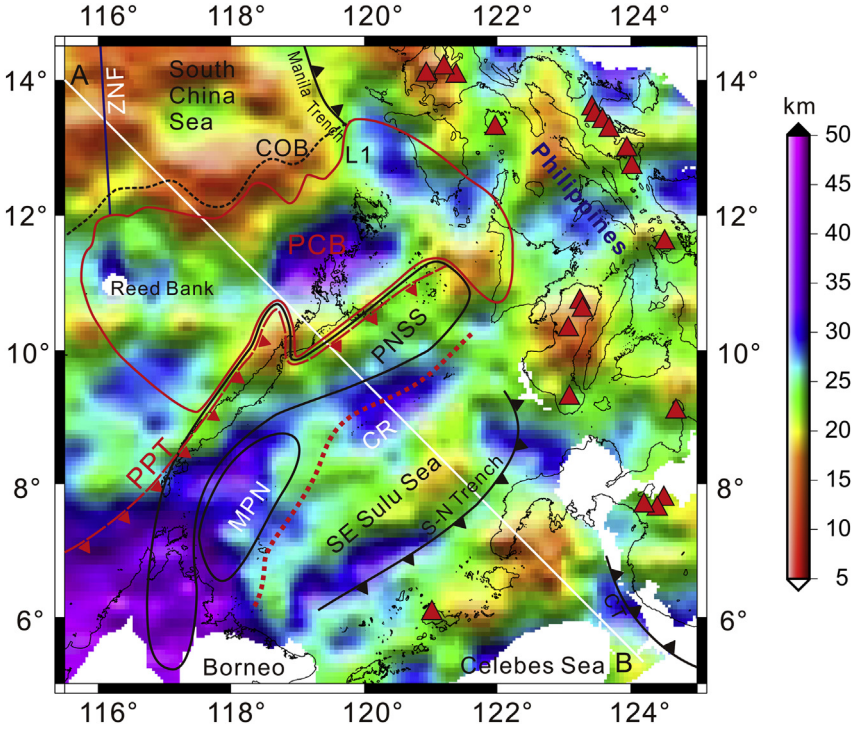

Figure 7. The average of Curie-point depths calculated from different window sizes. Transect AB is shown in Fig. 13 and see Figures 2, 3 and 6 for other notations.

window sizes, but generally the results of different window sizes have similar patterns (Figs. 8 and 9). Top of the magnetic layer has intermediate depths in the southern SCS continental margin, particularly around the Calamian Island Group (CIG) and south Palawan area. This observation is consistent with that made in their counterpart in the northern SCS margin (Li and Song, 2012). It is obvious that the Philippines and the Zamboanga Peninsula have the shallowest depths to the top of the magnetic layer, reflecting their island arc essence. The Philippines have numerous volcanoes caused by the subduction along the Manila, Philippine and Sulu-Negros Trenches. Almost all volcanoes active in recent 2000 years are seated in the regions of small depths to the top of magnetic sources. The SCS shows depths to the top of magnetic sources around 2–5 km, also consistent to its known depths to the oceanic basement. The hyper-extended continental crust (zone between COB and L1 in Figs. 8 and 9) shows large geothermal gradients from our estimated Curie depths.

Overall, from both Curie depths and depths to the top of magnetic sources, we find that the PCB is relatively quiet in magmatic activities and moderate in thermal gradients, and has a reasonable thickness of non-magnetic strata (Cenozoic and Mesozoic sedimentary rocks).

5. Inversion of 3D Moho topography

The free-air gravity anomaly data (Sandwell and Smith, 2009) (Fig. 10) and topography data (Becker et al., 2009) are used to invert the 3D Moho topography. We space both data based on 1-min gridding. Bouguer gravity anomalies (Fig. 11) are computed with the assumed correcting density of 2.67 g/cm^3 for the shallow crustal material. We find that the Bouguer gravity high, interpreted as an ophiolite complex in south Palawan and NE Sabah, also occupies part of the NW Sulu Sea (Fig. 11).

Bouguer gravity anomalies have been taken routinely to estimate the depth to the Moho, which represents the largest density contrast in the lithosphere (Dziewonski and Anderson, 1981) and contributes the most to surface Bouguer gravity anomalies (Woodside and Carl, 1970). The Parker–Oldenburg algorithm (Parker, 1973; Oldenburg, 1974) is efficient and straightforward in manipulating large datasets (Nagendra et al., 1996; Gómez-Ortiz and Agarwal, 2005; Shin et al., 2006). This algorithm is applied here to yield a 3D Moho topography, assuming that there is a constant density contrast of 0.5 g/cm^3 across the Moho and the long-wavelength anomalies are all from mantle undulations (Fig. 12). Iterative forward modeling of the gravity field (Parker, 1973) and inverse calculations of the Moho depth (Oldenburg, 1974) are applied until a prescribed converging criterion is reached.

Expectedly, thick crust is found in the zones of the PCB, Philippine Mobile Belt, NW Sulu Sea, Borneo and Sulu Arc. The seismically interpreted Moho is quite consistent with our inverted Moho depth from gravity (Fig. 5). Because of remaining uncertainties in the crustal ages of the SE Sulu Sea and Celebes Sea, we did not conduct lithospheric thermal correction before the Moho inversion. Thus, the older basin should show shallower apparent Moho for its denser crust. The apparent Moho from gravity inversion without the thermal correction appears to be the shallowest in the Celebes Sea, intermediate in the SE Sulu Sea, and deepest in the SCS (Figs. 12 and 13). The Celebes Sea is a middle Eocene oceanic basin identified by magnetic anomalies (Weissel, 1980), and ODP Leg 124 also confirmed this age (Silver and Rangin, 1991). The formation time of the SE Sulu Sea could be either the Early Miocene (Rangin and Silver, 1991) or the Oligocene (Roeser, 1991). From our apparent Moho depths, the Celebes Sea should be the oldest basin among the three basins, and the SE Sulu Sea should be older than the SCS. This

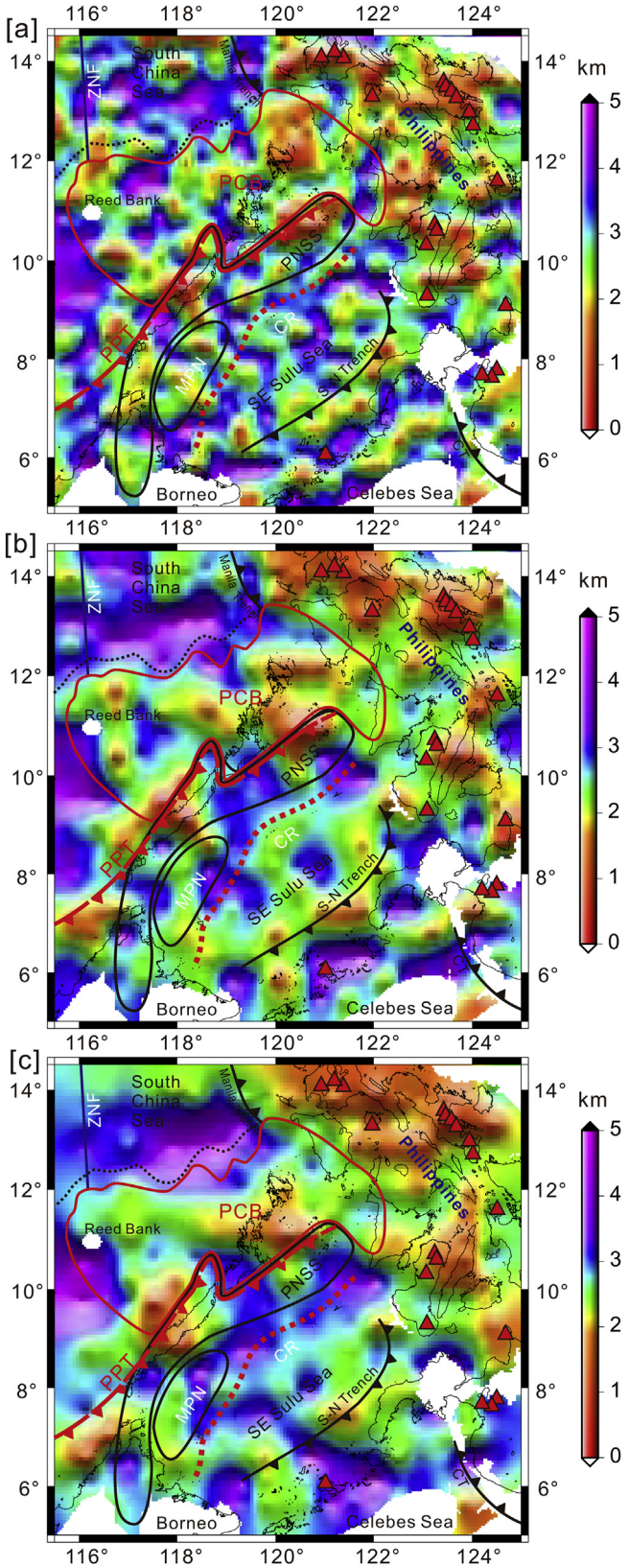

Figure 8. Maps of depths to the top of the magnetic layer estimated from using window sizes in 60 km × 60 km[a], 100 km × 100 km[b] and 150 km × 150 km[c]. See Figures 2, 3 and 6 for other notations.

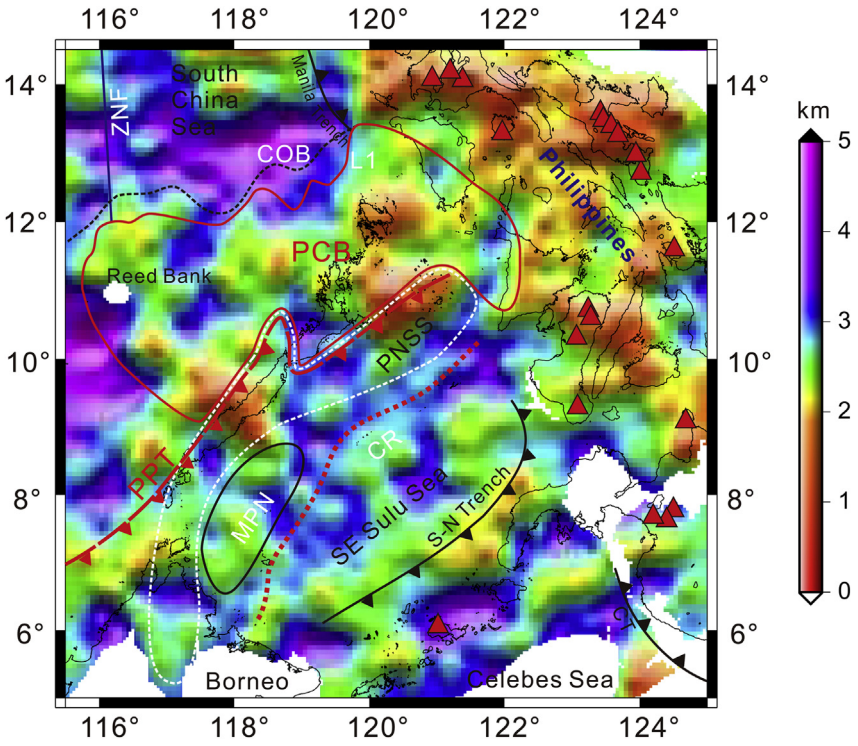

Figure 9. The average of depths to the top of the magnetic layer calculated from different window sizes. See Figures 2, 3 and 6 for other notations.

suggests that the Late Eocene – Early Oligocene opening of the SE Sulu Sea should be more reasonable.

In addition, a lower geothermal gradient is also expected in an older basin. The lower geothermal gradient in the SE Sulu Sea comparing with that of the SCS also suggests that the SE Sulu Sea is older than SCS. The lowest geothermal gradient appears in the Celebes Sea (Fig. 13). Therefore, the same age order of these three basins is concluded from both Moho and Curie-point depths.

6. Discussions

6.1. The PCB and extinct trench of the PSCS

The deep structural characteristics of PCB are quite different from the ambient region (Figs. 7 and 12). Differences in Moho and Curie-point depth are observed between the PCB and Borneo, indicating different origins of the two blocks. The eastern boundary

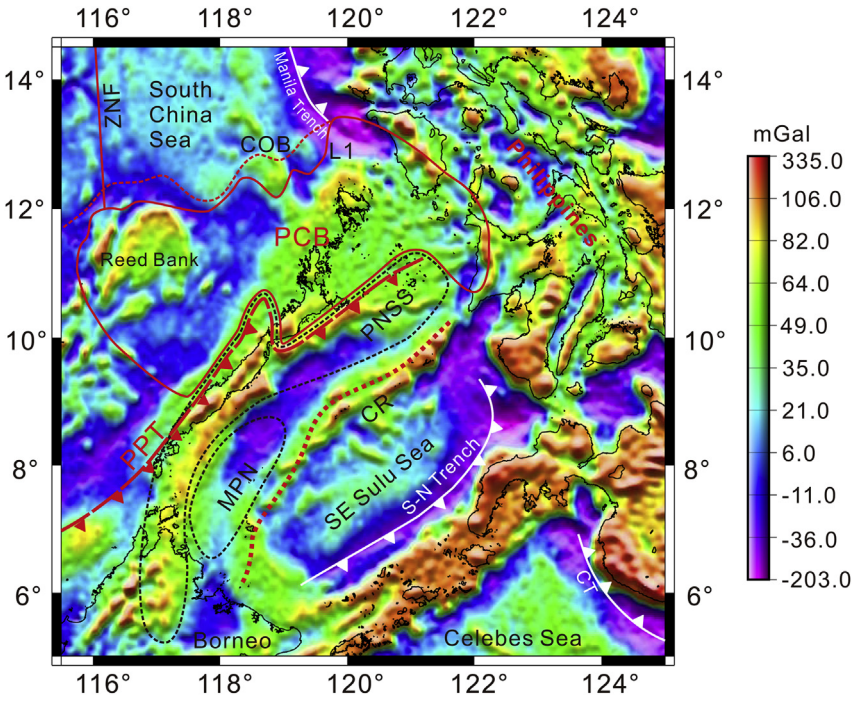

Figure 10. Regional map of free air gravity anomalies. Data are from Sandwell and Smith (2009). See Figures 2 and 3 for other notations.

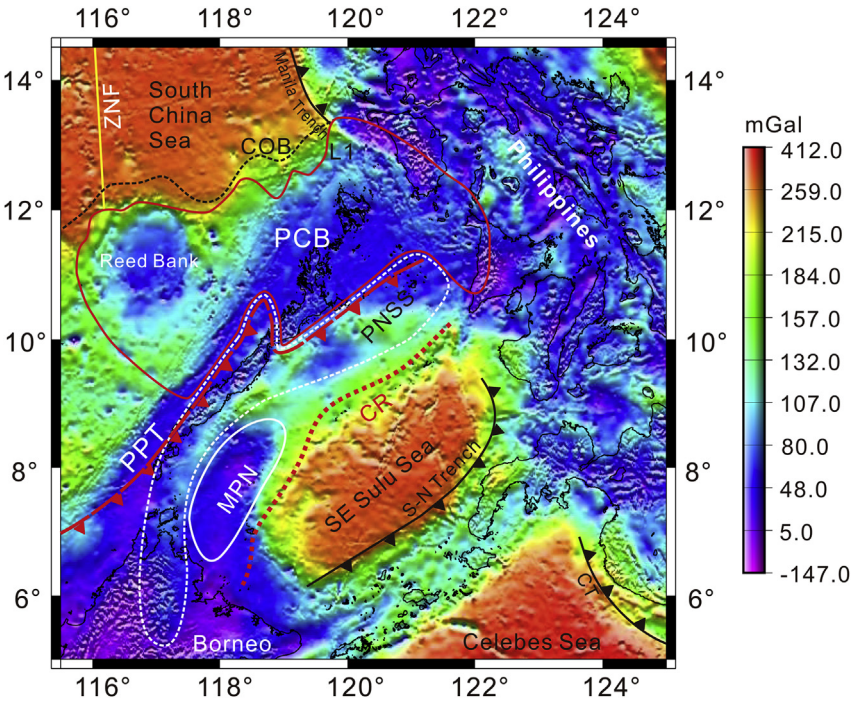

Figure 11. Regional map of Bouguer gravity anomalies. See Figures 2 and 3 for other notations.

of the PCB defined by the ASA and magnetic anomalies on the Mindoro and Panay Island is well consistent with results from the geological surveys (Sarewitz and Karig, 1986; Jumawan et al., 1998; Tamayo et al., 2001; Zamoras et al., 2008). The western boundary of the PCB is more prominent on a larger scale to the west of Reed Bank (Li and Song, 2012; Shi and Li, 2012). The serpentinized peridotite on the Paly Island and Dumaran Island (Fig. 2) is found in the outcrop or underlying the Late Cretaceous continental rocks (MMAJ-JICA, 1988; Aurelio and Peña, 2010), and is induced likely by the palaeo-Pacific subduction along the southern margin of Eurasia that took place from the Late Paleozoic to Late Mesozoic before the drifting of the PCB (Li and Li, 2007; Li et al., 2012). Significant quantities of aqueous fluid that released from the downgoing palaeo-Pacific oceanic crust may have hydrated the upper mantle

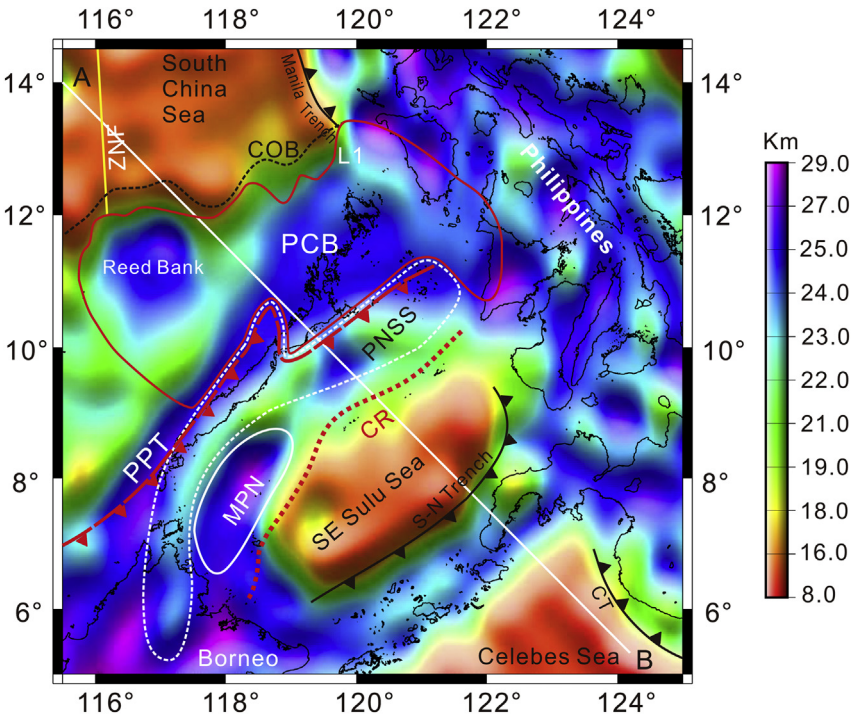

Figure 12. Estimated Moho topography from Bouguer anomalies. Transect AB is shown in Fig. 13 and see Figures 2 and 3 for other notations.

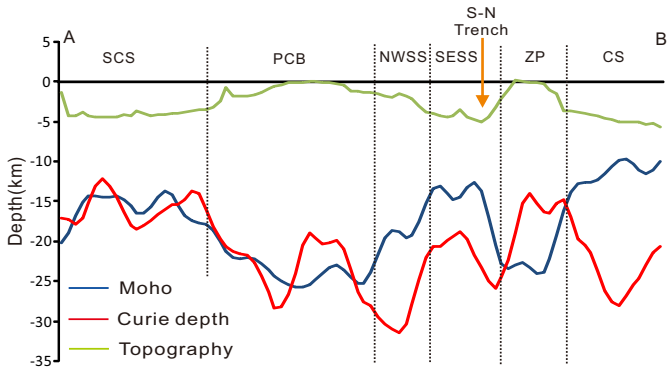

Figure 13. Geophysical transect AB (showing in Figs. 7 and 12). SCS = South China Sea, PCB = Palawan Continental Block, NWSS = NW Sulu Sea, SESS = SE Sulu Sea, S-N Trench = Sulu-Negros Trench, ZP = Zamboanga Peninsula, CS = Celebes Sea.

peridotite and triggered the serpentinization. That also demonstrates that the Paly Island and Dumaran Island are Eurasia originated and are situated on the margin of the PCB. The PCB itself is magnetically quieter and topographically flatter than surrounding blocks, and a remarkable geographical difference is shown along the western boundary of the PCB. In addition, the Zhongnan Fault (ZNF in Figures) may have affected and controlled the western boundary of the PCB.

The PSCS is assumed to be a pre-existing Late Cretaceous oceanic crust situated to the south of the Eurasian continent (Hall and Wilson, 2000; Hutchison et al., 2000; Hutchison, 2005; Hall et al., 2008; Hall, 2011), and it gradually closed along the southeast subduction zone with the opening of the SCS. It has been demonstrated that the Palawan Trough does not represent the location of an ancient subduction zone (Hinz and Schlüter, 1985; Milsom et al., 1997; Ingram et al., 2004; Hesse et al., 2009). Indeed, the seismic section (Fig. 5) crossing part of the Palawan Trough shows no signs of convergent but extensional structures of listric faults and half-grabens. It has been verified that the present Palawan Trough is not a subduction-related trench. We also confirm that the exact position of the extinct trench was located to the southeast of the present Palawan Trough (Fig. 4). Here, the extinct convergent margin for the PSCS is named the Proto Palawan Trench (PPT). Because of later obduction of relict oceanic slice onto the south Palawan, the original southern boundary of PCB and the paleo-trench for subduction of PSCS should have lied further south. We argue that the previous low bathymetry in Proto Palawan Trench was covered and concealed by the slab obducted onto the PCB.

6.2. *Range of the relict oceanic slice and nature of the NW Sulu Sea*

The ophiolite complex in south Palawan formed from the Late Cretaceous to Eocene (Raschka et al., 1985; Letouzey et al., 1988; Müller, 1991). An $^{39}Ar/^{40}Ar$ isochron age of 34 Ma (Late Eocene) is obtained from pillow basalts in south Palawan (Encarnación, 2004). Schlüter et al. (1996) speculated that the ophiolite complex in central and south Palawan was part of NW Sulu Sea overthrusted onto the Palawan. Based on the paleomagnetism of southern Palawan, the ophiolite complex had a paleolatitude near the present Celebes Sea and underwent a counterclockwise rotation, northward displacement and obduction during the Eocene and Oligocene (Almasco et al., 2000). The joint ophiolitic basement of south Palawan and NE Sabah has been confirmed from Bouguer gravity anomalies (Cullen et al., 2010). These former studies have put the origin of south Palawan, NE Sabah and NW Sulu Sea quite different from that of the PSCS. We also infer that south Palawan, NE Sabah and NW Sulu Sea sourced from a southern relict block, although the exact extent of the relict oceanic slice is obscure.

The nearly N–S trending Ulugan Bay fault (Figs. 2 and 4) represents the boundary between the north and south Palawan (Yumul et al., 2009) and corresponds to a line of high ASA contrast. ASA depends on the volumes and depths of magnetic sources, Earth's magnetic field intensities, and the susceptibilities of magmatic rocks (Shi and Li, 2012). We interpret that the high ASA of south Palawan is caused by the ophiolite complex, which extends northeastward into the NW Sulu Sea and southward into Sabah (Fig. 4) and shows high Bouguer gravity anomalies (Fig. 11). For those reasons, we consider the entire high ASA zone, covering the south Palawan, NE Sabah and part of NW Sulu Sea (Fig. 4), to be the relict oceanic crust, which experienced the same counterclockwise rotation and northward migration during the Eocene and Oligocene as did the ophiolite complex of south Palawan. Furthermore, because the oceanic rock formations (the Palawan Ophiolite Complex) are exposed in the south Palawan and the boundary between the north and south Palawan is defined by the Ulugan Bay fault (Raschka et al., 1985; Letouzey et al., 1988; Faure et al., 1989; Müller, 1991; Fuller et al., 1991; Encarnación, 2004; Yumul et al., 2009), the northeast boundary of the high ASA zone of south Palawan is regarded as the Ulugan Bay fault (Fig. 4). Hereafter the term Proto NW Sulu Sea is used to refer the relict oceanic crust (PNSS in Fig. 4). The thick sedimentary sequences overlying the ophiolitic basement in NE Sabah (Jackson et al., 2009) induce relatively lower ASA comparing with that in south Palawan and NW Sulu Sea.

The present-day crustal thickness of the Proto NW Sulu Sea is much larger than that of a typical oceanic basin (Figs. 12 and 13). We attribute this large thickness to the obduction of the Proto NW Sulu Sea onto the PCB. When continental crust of the PCB, following the PSCS plate, entered the trench, the oceanic slab of the PSCS detached and descended into the mantle, and then the continental crust ascended and clung to the bottom of Proto NW Sulu Sea plate due to isostasy. The detachment of the PSCS has been suggested by tomographic study (Rangin et al., 1999).

Two obduction events occurred in different parts of the Proto NW Sulu Sea. The first is that the southwest portion of Proto NW Sulu Sea obducted onto the NE Sabah in the Late Eocene and accounts for the ophiolitic basement of NE Sabah (Omang and Barber, 1996). The Proto NW Sulu Sea and Sabah formed a rigid block and rotated together (Hall, 1996, 2002; Fuller et al., 1999). The second event is the obduction of the Proto NW Sulu Sea onto the PCB at the end of subduction of the PSCS, leading to the emplacement of onland ophiolite of south Palawan (Schlüter et al., 1996; Almasco et al., 2000). According to the timing of cessation of deformation in the NW Sulu Sea (Rangin and Silver, 1991), the obduction of Proto NW Sulu Sea ceased in the Middle Miocene. Although the Proto NW Sulu Sea and the PSCS were proximal to each other in the Eocene because of their respective movements, they are differently originated blocks. The Proto NW Sulu Sea is a relict Late Cretaceous to Eocene oceanic slice originated from further south, not coherent to the northerly PSCS (Fig. 14). Furthermore, the simultaneous collision between PCB and Philippine Mobile Belt (Yumul et al., 2009) caused thickened crust along the eastern boundary of the PCB (Fig. 12). In addition, the original bathymetric low in the PPT disappeared and is indistinct at its present location, resulting from the obduction of the Proto NW Sulu Sea onto the PCB.

With the confirmed range of a relict oceanic crust, and with the evident differences in ASA, Curie-point and Moho depths, and Bouguer gravity anomalies between the southwest part of the NW Sulu Sea (area of "MPN") and the Proto NW Sulu Sea (area of "PNSS") (Figs. 4, 7, 11, and 12), we infer the southwest part of the NW Sulu Sea to be the relict margin of the Proto NW Sulu Sea,

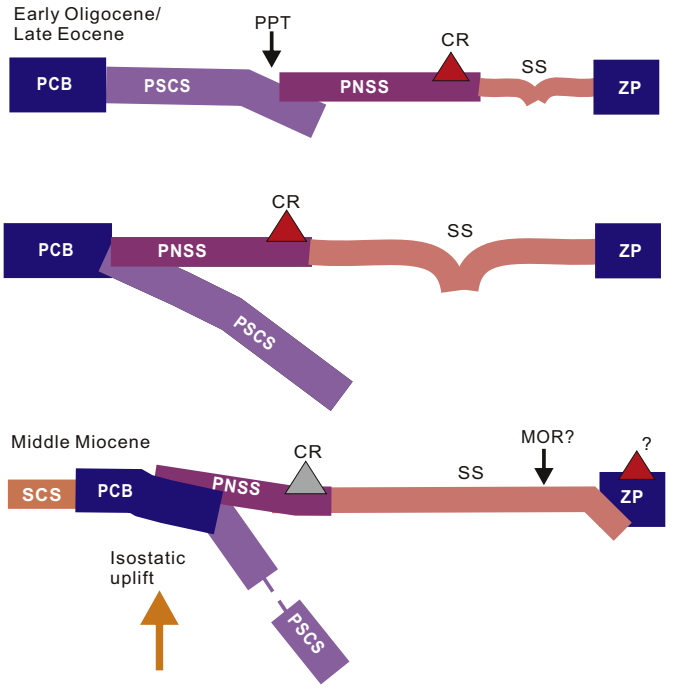

Figure 14. Evolution model for the SE Sulu Sea. PCB = Palawan continental block, PSCS = Proto South China Sea, PPT = Proto Palawan Trench, PNSS = Proto NW Sulu Sea, CR = Cagayan Ridge, SS = SE Sulu Sea, MOR = Middle Ocean Ridge, ZP = Zamboanga Peninsula.

where relatively larger Moho depth and lower Bouguer gravity anomalies are expected (Figs. 11 and 12). The whole NW Sulu Sea is concluded to be a southerly originated block, most of which has an ophiolitic basement formed from the Late Cretaceous to Eocene.

Moreover, the ASA in the Proto NW Sulu Sea shows an apparent NEE trending pattern (Fig. 4), which might be parallel to the spreading center of the Proto NW Sulu Sea. Perpendicular to the linear ASA zone, the Ulugan Bay fault is interpreted as a relict transform fault of the Proto NW Sulu Sea. Due to the lower resolution of potential field data, the exact position and trending of the Ulugan Bay Fault in our interpretation may be slightly different from some of earlier studies, especially onshore geological studies (e.g. Hamilton, 1979; Roberts, 1983; Suzuki et al., 2000b). The contrasting characteristics in Moho depths, Curie-point depths and Bouguer anomalies between the PCB-NW Sulu Sea and Borneo suggest that these two blocks are of different origins.

6.3. Hydrocarbon potential of the PCB

As mentioned earlier, the PCB was adjacent to the Chaoshan Depression and Tainan Basin located in the northern margin of SCS before opening of the SCS (Fig. 1) (Holloway, 1982; Taylor and Hayes, 1983; Suzuki et al., 2000b; Shi and Li, 2012). Prior to the opening of SCS, the Mesozoic strata in the PCB deposited in the same tectonic setting as those of the Chaoshan Depression and Tainan Basin.

Based on gravimetric, magnetic, seismic, and lithofacies data, Shi and Li (2012) identified three major phases of Mesozoic marine deposition in two large areas of the northern South China Sea margin. They are the Paleozoic and Early Triassic sequences within a mostly Tethyan affiliation, the Late Triassic to Early Jurassic palaeo-Pacific transgression with coastal to shallow marine clastic deposits, and the Middle Jurassic to the Early Cretaceous forearc deposition along the palaeo-Pacific subduction zone. Despite strong late-stage rifting and magmatism in the region, Mesozoic marine sedimentary strata are well preserved and can be traced all the way to the continent–ocean boundary (Shi and Li, 2012).

The same suite of Mesozoic sedimentary strata is expected in the southern margin of SCS. Similar to the northern margin, three Mesozoic stratigraphic sections have been shown from more than 10 wells drilled in the PCB area, i.e., Lower Cretaceous–Upper Jurassic, Lower Jurassic–Upper Triassic and mid-Triassic (Taylor and Hayes, 1980, 1983). Especially in the SE Reed Bank, the Lower Cretaceous and Jurassic strata are up to 5000 m thick (Taylor and Hayes, 1980).

Like the PCB, the Chaoshan Depression and Tainan Basin are also magnetically quiet and are underlain by thick Mesozoic sedimentary rocks (Shi and Li, 2012; Li and Song, 2012). It is found that both Mesozoic and Cenozoic magmatic activities generally subside southeastward, and the southern part had a longer period of deep Tethyan and Pacific marine deposition (Shi and Li, 2012), making the hydrocarbon potential of the PCB even more favorable than in the Chaoshan Depression and Tainan Basin.

Magnetic data of the PCB show it has very weak Mesozoic and Cenozoic volcanic activities (Fig. 4) and remained tectonically uniform during the Cenozoic. The PCB has moderate depths to Curie points and top of magnetic sources. We further interpret that the PCB is underlain with thick Mesozoic sedimentary rocks of marine facies that are of economic importance. Similar characteristics in the Mesozoic strata between the Chaoshan Depression and Reed Bank Basin are revealed by reflection seismic profiles (Sun et al., 2008; Yao et al., 2012). Commercial petroleum reservoirs, sourced from the Mesozoic strata, are found in the Tainan Basin (He et al., 2006). Considerable total organic carbon content in the Lower Cretaceous strata is also found in the Sampaguita-1 well in the Reed Bank (e.g., Xia and Huang, 2000; Williams, 1997). Since the Chaoshan Depression and Tainan Basin show relatively high thermal maturity for the Mesozoic source rocks (He et al., 2006), the Mesozoic sequences in PCB are also expected to be thermally mature for oil and gas generation.

Seismic interpretation of Cenozoic strata in the PCB demonstrates that the Cenozoic has a maximum thickness exceeding 6000 m in the Reed Bank Basin (Yao et al., 2012). The Reed Bank Basin received a sedimentary sequence of clastic rocks and carbonate rocks of marine facies during the Cenozoic. It is suggested that the Paleocene to Lower Oligocene was the most favorable period for the development of source rocks in northwest Palawan (Sales et al., 1997). The period of post-seafloor spreading of SCS is the stage for development of coral reefs (Yao et al., 2012), which form a number of proven Cenozoic exploration plays (Williams, 1997; Sales et al., 1997). Thereby, the PCB is a potentially favorable block for both Mesozoic and Cenozoic hydrocarbon explorations.

6.4. The evolution model of the Sulu Sea

Two evolutional model of the SE Sulu Sea were presented, either as a back-arc basin triggered by subduction of the PSCS (Rangin and Silver, 1991) or Celebes Sea plate (Rangin, 1989), or a marginal basin similar to the SCS (Rangin and Silver, 1991). Besides, the formation time of the SE Sulu Sea, either the Early Miocene (Rangin and Silver, 1991) or the Oligocene (Roeser, 1991), is also in debate.

From the Moho and Curie-point depths, the SE Sulu Sea should be older than the SCS. Based on the back-arc basin hypothesis supported by geochemical signatures (Rangin and Silver, 1991), the formation time of the SE Sulu Sea is supposed to be close to that of the associated volcanic arc. The Cagayan Ridge, as the volcanic arc paired with the extinct trench, formed by the subduction of the PSCS that commenced from Eocene (Hamilton, 1979; Rangin et al.,

1990; Lee and Lawver, 1995; Hall, 1996; Hutchison et al., 2000). The Cagayan Ridge was dated to be 33.9 ± 7.7 Ma from apatite fission track (Hutchison et al., 2000). Our magnetic studies around the Cagayan Ridge support for its old age, because the ridge today is not accompanied with significantly shallower Curie points or tops to magnetic sources, as would be expected along a young and active volcanic arc. The SE Sulu Sea was suggested to be a Late Oligocene basin from the interpretation of magnetic anomalies (Roeser, 1991), however, the magnetic anomalies are not convincingly recognized so far and are no longer intact owing to the subduction along the Sulu Trench and Negros Trench respectively. We suggest that the initial spreading of the SE Sulu Sea occurred in the Early Oligocene or Late Eocene.

It should be noted that our constraint on the age of the SE Sulu Sea oceanic crust is based on the estimated Curie depths that offer insight on the lithospheric temperatures and therefore the relative ages. Curie depths are estimated from magnetic anomalies, but are independent of age determinations directly from magnetic anomaly correlations with the Global Magnetic Polarity Reversal Scale. We here have provided an independent, albeit less direct, geophysical method to constrain the relative age of the SE Sulu Sea in relation to those of the SCS and Celebes Sea.

We favor a modified back-arc evolution model of the SE Sulu Sea (Fig. 14), for geological similarity in basement between the NW Sulu Sea to the north and Zamboanga Peninsula to the south. The basement rocks in Zamboanga Peninsula, including slivers of Late Cretaceous ophiolitic rocks (Pubellier et al., 2004), are consistent with the nature of the NW Sulu Sea we concluded above. In the Early Oligocene/Late Eocene, the back-arc spreading, paired with Cagayan Ridge arc volcanism, started from the subduction of the PSCS along the PPT. The volcanic activities of the Cagayan Ridge and seafloor spreading of the SE Sulu Sea continued until the detachment of the PSCS slab and obduction of the Proto NW Sulu Sea onto the south Palawan in the Middle Miocene. This timing fits well with the cessation of deformation in the NW Sulu Sea (Rangin and Silver, 1991). The subduction of the SE Sulu Sea occurred in the Middle Miocene (Pubellier et al., 1991; Rangin and Silver, 1991), likely due to the collision between the PCB and Proto NW Sulu Sea.

7. Conclusion

The uniform Palawan Continental Block (PCB) is characterized by a magnetically quiet zone from ASA and total field magnetic anomalies. The continent–ocean boundary (COB) between the PCB and SCS is discriminated by the Moho depth and Bouguer gravity anomalies and is confirmed by recently acquired reflection seismic data. With further constraints from Moho inversion, we find that the northern boundary of the PCB identified from magnetic data does not coincide with the COB, because there is a narrow zone of hyper-extended continental crust with intense magmatism that induce strong magnetic anomalies. Therefore the COB is located slightly further north, coincidental in many places, though not always, with the seaward limit of a zone of low free-air gravity anomalies. The regional distribution of hyper-extended continental crust needs to be further investigated to better understand the early opening of the SCS.

The PCB is considered as a favorable block for hydrocarbon exploration, due to its thick Mesozoic deposition, weak Mesozoic and Cenozoic magmatic activities, and moderate geothermal gradient and depths to the magnetic top. From the identified boundary of the PCB, the present geometry and position of the extinct convergent margin of the PSCS is confirmed to coincide with the southern boundary of the PCB, being located partially to the southeast of the north Palawan and partially to the northwest of the south Palawan. The NW Sulu Sea is found to be a thickened relict oceanic slice that obducted onto SE Sabah in the late Eocene and subsequently onto the south Palawan in the Middle Miocene. The Ulugan Bay fault is inferred to be a relict transform fault developed initially within the Proto NW Sulu Sea. Our estimated Moho and Curie-point depths give an independent constraint on the age order of the Celebes Sea, SE Sulu Sea and SCS; the SE Sulu Sea should be younger than the Celebes Sea but older than the SCS, most likely with a Late Eocene – Early Oligocene age.

We propose a modified evolution model for the SE Sulu Sea. Different from the back-arc evolution models presented previously, we suggest that the SE Sulu Sea was a back-arc basin formed in the Early Oligocene/Late Eocene, and the Proto NW Sulu Sea formed from the Late Cretaceous to Eocene between the Proto Palawan Trench and the Cagayan Ridge.

Acknowledgments

Data processing is supported by the USGS potential field software (Cordell et al., 1993; Phillips, 1997), and by GMT (Wessel and Smith, 1995). This research is funded by National Natural Science Foundation of China (Grants 91028007), Program for New Century Excellent Talents in University (NCET-10-0601), and Research Fund for the Doctoral Program of Higher Education of China (Grant 20100072110036). We thank two anonymous reviewers for their detailed comments.

References

Agarwal, B.N.P., Shaw, R.K., 1996. Comment on 'An analytic signal approach to the interpretation of total field magnetic anomalies' by Shuang Qin. Geophys. Prospect. 44, 911–914.
Agrawal, P., Thakur, N., Negi, J., 1992. MAGSAT data and Curie-depth below Deccan flood basalts (India). Pure Appl. Geophys. 138, 61–75.
Almasco, J., Rodolfo, K., Fuller, M., Frost, G., 2000. Paleomagnetism of Palawan, Philippines. J. Asian Earth Sci. 18, 369–389.
Aurelio, M.A., Peña, R.E. (Eds.), 2010. Geology of the Philippines, Tectonics and Stratigraphy, vol. 1. Mines and Geosciences Bureau, Department of Environment and Natural Resources, Quezon City, Philippines.
Aurelio, M.A., Peña, R.E., Taguibao, K.J.L., 2012. Sculpting the Philippine archipelago since the Cretaceous through rifting, oceanic spreading, subduction, obduction, collision and strike-slip faulting: contribution to IGMA5000. J. Asian Earth Sci. 72, 102–107.
Becker, J., Sandwell, D., Smith, W., Braud, J., Binder, B., Depner, J., Fabre, D., Factor, J., Ingalls, S., Kim, S., 2009. Global bathymetry and elevation data at 30 arc seconds resolution: SRTM30_PLUS. Mar. Geod. 32, 355–371.
Blakely, R.J., 1996. Potential Theory in Gravity and Magnetic Applications. Cambridge University Press.
Bouligand, C., Glen, J.M., Blakely, R.J., 2009. Mapping Curie temperature depth in the western United States with a fractal model for crustal magnetization. J. Geophys. Res. 114, B11104. http://dx.doi.org/10.1029/2009JB006494.
Briais, A., Patriat, P., Tapponnier, P., 1993. Updated interpretation of magnetic anomalies and seafloor spreading stages in the South China Sea: implications for the Tertiary tectonics of Southeast Asia. J. Geophys. Res. 98, 6299–6328.
Castillo, P., Rigby, S., Solidum, R., 2007. Origin of high field strength element enrichment in volcanic arcs: geochemical evidence from the Sulu Arc, southern Philippines. Lithos 97, 271–288.
Geological Survey of Japan and Coordinating Committee for Coastal and Offshore Geoscience Programmes in East and Southeast Asia (CCOP), 1996. Magnetic Anomaly Map of East Asia 1:4,000,000. CD-ROM Version.
Cordell, L., Phillips, J.D., Godson, R.H., 1993. USGS potential-field geophysical software for PC and compatible microcomputers. Lead. Edge 12, 290.
Cullen, A.B., 2010. Transverse segmentation of the Baram-Balabac Basin, NW Borneo: refining the model of Borneo's tectonic evolution. Pet. Geosci. 16, 3–29.
Cullen, A., Reemst, P., Henstra, G., Gozzard, S., Ray, A., 2010. Rifting of the South China Sea: new perspectives. Pet. Geosci. 16, 273–282.
Ding, W.-W., Li, J.-B., 2011. Seismic stratigraphy, tectonic structure and extension factors across the southern margin of the South China Sea: evidence from two regional multi-channel seismic profiles. Chin. J. Geophys. 54, 3038–3056 (in Chinese).
Dziewonski, A.M., Anderson, D.L., 1981. Preliminary reference Earth model. Phys. Earth Planet. Inter. 25, 297–356.
Encarnación, J., 2004. Multiple ophiolite generation preserved in the northern Philippines and the growth of an island arc complex. Tectonophysics 392, 103–130.

Faure, M., Marchadier, Y., Rangin, C., 1989. Pre-Eocene synmetamorphic structure in the Mindoro-Romblon-Palawan area, west Philippines, and implications for the history of southeast Asia. Tectonics 8, 963–979.
Fontaine, H., 1979. Note on the geology of the Calamian islands, North Palawan, Philippines. CCOP Newsl. 6, 40–46.
Franke, D., Barckhausen, U., Heyde, I., Tingay, M., Ramli, N., 2008. Seismic images of a collision zone offshore NW Sabah/Borneo. Mar. Pet. Geol. 25, 606–624.
Franke, D., Barckhausen, U., Baristeas, N., Engels, M., Ladage, S., Lutz, R., Montano, J., Pellejera, N., Ramos, E.G., Schnabel, M., 2011. The continent-ocean transition at the southeastern margin of the South China Sea. Mar. Pet. Geol. 28, 1187–1204.
Fuller, M., Haston, R., Lin, J.-I., Richter, B., Schmidtke, E., Almasco, J., 1991. Tertiary paleomagnetism of regions around the South China Sea. J. Southeast Asian Earth Sci. 6, 161–184.
Fuller, M., Ali, J.R., Moss, S.J., Frost, G.M., Richter, B., Mahfi, A., 1999. Paleomagnetism of Borneo. J. Asian Earth Sci. 17, 3–24.
Gómez-Ortiz, D., Agarwal, B.N., 2005. 3DINVER.M: a MATLAB program to invert the gravity anomaly over a 3D horizontal density interface by Parker–Oldenburg's algorithm. Comput. Geosci. 31, 513–520.
Hall, R., 1996. Reconstructing Cenozoic SE Asia. In: Geological Society, London, Special Publications, vol. 106, pp. 153–184.
Hall, R., 2002. Cenozoic geological and plate tectonic evolution of SE Asia and the SW Pacific: computer-based reconstructions, model and animations. J. Asian Earth Sci. 20, 353–431.
Hall, R., 2011. Australia–SE Asia Collision: Plate Tectonics and Crustal Flow. In: Geological Society, London, Special Publications, vol. 355, pp. 75–109.
Hall, R., Wilson, M., 2000. Neogene sutures in eastern Indonesia. J. Asian Earth Sci. 18, 781–808.
Hall, R., van Hattum, M.W., Spakman, W., 2008. Impact of India–Asia collision on SE Asia: the record in Borneo. Tectonophysics 451, 366–389.
Hamilton, W.B., 1979. Tectonics of the Indonesian Region. US Govt. Print. Off.
He, J., Xia, B., Wang, Z., Sun, D., 2006. Petroleum geologic characteristics and exploration base of Taixinan Basin in eastern area of continental shelf in northern of the South China Sea. Nat. Gas. Geosci. 17, 345–350 (in Chinese).
Hesse, S., Back, S., Franke, D., 2009. The deep-water fold-and-thrust belt offshore NW Borneo: gravity-driven versus basement-driven shortening. Geol. Soc. Am. Bull. 121, 939–953.
Hinz, K., Block, M., 1990. Summary of geophysical data from the Sulu and Celebes Seas. In: Rangin, C., Silver, E.A., von Breymann, M.T., et al. (Eds.), Proc. ODP, Init. Repts, pp. 87–92.
Hinz, K., Schlüter, H., 1985. Geology of the dangerous grounds, South China sea, and the continental margin off southwest Palawan: results of SONNE cruises SO-23 and SO-27. Energy 10, 297–315.
Hinz, K., Fritsch, J., Kempter, E., Mohammad, M.A.M., Meyer, J., Mohamed, M.D., Vosberg, D.G.H., Weber, D.I.J., Benavidez, M.J., 1989. Thrust tectonics along the north-western continental margin of Sabah/Borneo. Geol. Rundsch. 78, 705–730.
Holloway, N., 1982. North Palawan block, Philippines–Its relation to Asian mainland and role in evolution of South China Sea. AAPG Bull. 66, 1355–1383.
Huismans, R., Beaumont, C., 2011. Depth-dependent extension, two-stage breakup and cratonic underplating at rifted margin. Nature 473, 74–78.
Hutchison, C.S., 2005. Geology of North-West Borneo: Sarawak, Brunei and Sabah. Elsevier Science.
Hutchison, C.S., Bergman, S.C., Swauger, D.A., Graves, J.E., 2000. A Miocene collisional belt in north Borneo: uplift mechanism and isostatic adjustment quantified by thermochronology. J. Geol. Soc. 157, 783–793.
Ingram, G., Chisholm, T., Grant, C., Hedlund, C., Stuart-Smith, P., Teasdale, J., 2004. Deepwater North West Borneo: hydrocarbon accumulation in an active fold and thrust belt. Mar. Pet. Geol. 21, 879–887.
Jackson, C.A.L., Zakaria, A.A., Johnson, H.D., Tongkul, F., Crevello, P.D., 2009. Sedimentology, stratigraphic occurrence and origin of linked debrites in the West Crocker Formation (Oligo-Miocene), Sabah, NW Borneo. Mar. Pet. Geol. 26, 1957–1973.
Jumawan, F., Yumul Jr., G., Tamayo Jr., R., 1998. Using geochemistry as a tool in determining the tectonic setting and mineralization potential of an exposed upper mantle-crust sequence: example from the Amnay Ophiolitic Complex in Occidental Mindoro, Philippines. J. Geol. Soc. Philipp. 53, 24–48.
Lee, T.-Y., Lawver, L.A., 1995. Cenozoic plate reconstruction of Southeast Asia. Tectonophysics 251, 85–138.
Letouzey, J., Sage, L., Muller, C., 1988. Geological and Structural Map of Eastern Asia: Introductory Notes. American Association of Petroleum Geologists, Tulsa, OK.
Li, C.-F., 2005. Methods of mapping the depth to the Curie isotherm. Prog. Geophys. 20, 550–557.
Li, X., 2006. Understanding 3D analytic signal amplitude. Geophysics 71, L13–L16.
Li, Z.-X., Li, X.-H., 2007. Formation of the 1300-km-wide intracontinental orogen and postorogenic magmatic province in Mesozoic South China: a flat-slab subduction model. Geology 35, 179–182.
Li, C.-F., Song, T., 2012. Magnetic recording of the Cenozoic oceanic crustal accretion and evolution of the South China Sea basin. Chin. Sci. Bull. 57, 3165–3181.
Li, C.-F., Zhou, Z., Li, J., Hao, H., Geng, J., 2007. Structures of the northeasternmost South China Sea continental margin and ocean basin: geophysical constraints and tectonic implications. Mar. Geophys. Res. 28, 59–79.
Li, C.-F., Zhou, Z., Li, J., Chen, B., Geng, J., 2008. Magnetic zoning and seismic structure of the South China Sea ocean basin. Mar. Geophys. Res. 29, 223–238.
Li, C.-F., Chen, B., Zhou, Z., 2009. Deep crustal structures of eastern China and adjacent seas revealed by magnetic data. Sci. China (Ser. D) 52, 984–993.
Li, C.-F., Shi, X., Zhou, Z., Li, J., Geng, J., Chen, B., 2010. Depths to the magnetic layer bottom in the South China Sea area and their tectonic implications. Geophys. J. Int. 182, 1229–1247.
Li, X.-H., Li, Z.-X., He, B., Li, W.-X., Li, Q.-L., Gao, Y., Wang, X.-C., 2012. The Early Permian active continental margin and crustal growth of the Cathaysia Block: *In situ* U–Pb, Lu–Hf and O isotope analyses of detrital zircons. Chem. Geol. 328, 195–207.
Li, C.-F., Wang, J., Lin, J., Wang, T., 2013. Thermal evolution of the North Atlantic lithosphere: new constraints from magnetic anomaly inversion with a fractal magnetization model. Geochem. Geophys. Geosyst. 14, 5078–5105. http://dx.doi.org/10.1002/2013GC004896.
MacLeod, I.N., Jones, K., Dai, T.F., 1994. 3-D analytic signal in the interpretation of total magnetic field data at low magnetic latitudes. Explor. Geophys. 24, 679–688.
Maus, S., Dimri, V., 1994. Scaling properties of potential fields due to scaling sources. Geophys. Res. Lett. 21, 891–894.
Maus, S., Gordon, D., Fairhead, D., 1997. Curie-temperature depth estimation using a self-similar magnetization model. Geophys. J. Int. 129, 163–168.
Milsom, J., Holt, R., Ayub, D.B., Smail, R., 1997. Gravity Anomalies and Deep Structural Controls at the Sabah-Palawan Margin, South China Sea. In: Geological Society, London, Special Publications, vol. 126, pp. 417–427.
Mitchell, A., Leach, T., 1991. Epithermal Gold in the Philippines: Island Arc Metallogenesis, Geothermal Systems and Geology. Academic Press.
MMAJ-JICA: Metal Mining Agency of Japan – Japan International Cooperation Agency, November, 1988. Report on the Mineral Exploration: Mineral Deposits and Tectonics of Two Contrasting Geologic Environments in the Republic of the Philippines – Palawan V–VI, Area, West Negros Area and Samar I–IIII Area (1988), p. 347. Report submitted by MMAJ-JICA to the Republic of the Philippines.
Morley, C., 2002. A tectonic model for the Tertiary evolution of strike–slip faults and rift basins in SE Asia. Tectonophysics 347, 189–215.
Müller, C., 1991. Biostratigraphy and geological evolution of the Sulu Sea and surrounding area. In: Proceedings of the Ocean Drilling Program, Scientific Results, pp. 121–131.
Nabighian, M.N., 1972. The analytic signal of two-dimensional magnetic bodies with polygonal cross-section: its properties and use for automated anomaly interpretation. Geophysics 37, 507–517.
Nabighian, M.N., 1984. Toward a three-dimensional automatic interpretation of potential field data via generalized Hilbert transforms: fundamental relations. Geophysics 49, 780–786.
Nagao, T., Uyeda, S., 1995. Heat-flow distribution in Southeast Asia with consideration of volcanic heat. Tectonophysics 251, 153–159.
Nagendra, R., Prasad, P., Bhimasankaram, V., 1996. Forward and inverse computer modeling of a gravity field resulting from a density interface using Parker–Oldenberg method. Comput. Geosci. 22, 227–237.
Ofoegbu, C., Mohan, N., 1990. Interpretation of aeromagnetic anomalies over part of Southeastern Nigeria using three-dimensional Hilbert transformation. Pure Appl. Geophys. 134, 13–29.
Okubo, Y., Graf, R., Hansen, R., Ogawa, K., Tsu, H., 1985. Curie point depths of the island of Kyushu and surrounding areas, Japan. Geophysics 50, 481–494.
Oldenburg, D.W., 1974. The inversion and interpretation of gravity anomalies. Geophysics 39, 526–536.
Omang, S.A., Barber, A., 1996. Origin and Tectonic Significance of the Metamorphic Rocks Associated with the Darvel Bay Ophiolite, Sabah, Malaysia. In: Geological Society, London, Special Publications, vol. 106, pp. 263–279.
Parker, R., 1973. The rapid calculation of potential anomalies. Geophys. J. R. Astron. Soc. 31, 447–455.
Phillips, J.D., 1997. Potential-field Geophysical Software for the PC, Version 2.2. US Department of the Interior, US Geological Survey.
Pubellier, M., Quebral, R., Rangin, C., Deffontaines, B., Muller, C., Butterlin, J., Manzano, J., 1991. The Mindanao collision zone: a soft collision event within a continuous Neogene strike-slip setting. J. Southeast Asian Earth Sci. 6, 239–248.
Pubellier, M., Monnier, C., Maury, R., Tamayo, R., 2004. Plate kinematics, origin and tectonic emplacement of supra-subductionophiolites in SE Asia. Tectonophysics 392, 9–36.
Rangin, C., 1989. The Sulu Sea, a back-arc basin setting within a Neogene collision zone. Tectonophysics 161, 119–141.
Rangin, C., Silver, E.A., 1991. Neogene tectonic evolution of the Celebes-Sulu basins: new insights from Leg 124 drilling. In: Proc. ODP Sci. Results, 124, pp. 51–63.
Rangin, C., Bellon, H., Benard, F., Letouzey, J., Muller, C., Sanudin, T., 1990. Neogene arc-continent collision in Sabah, northern Borneo (Malaysia). Tectonophysics 183, 305–319.
Rangin, C., Spakman, W., Pubellier, M., Bijwaard, H., 1999. Tomographic and geological constraints on subduction along the eastern Sundaland continental margin (South-East Asia). Bull. Soc. géol. Fr. 170, 775–788.
Raschka, H., Nacario, E., Rammlmair, D., Samonte, C., Steiner, L., 1985. Geology of the ophiolite of central Palawan Island, Philippines. Ofioliti 10, 375–390.
Ravat, D., Pignatelli, A., Nicolosi, I., Chiappini, M., 2007. A study of spectral methods of estimating the depth to the bottom of magnetic sources from near-surface magnetic anomaly data. Geophys. J. Int. 169, 421–434.
Replumaz, A., Tapponnier, P., 2003. Reconstruction of the deformed collision zone between India and Asia by backward motion of lithospheric blocks. J. Geophys. Res. 108 http://dx.doi.org/10.1029/2001JB000661.

Roberts, M., 1983. Wrench Fault Tectonics: Seismic Example of Complex Faulting from Northwest Shelf of Palawan, Philippines, pp. 18–24.
Roeser, H., 1991. Age of the crust of the southeast Sulu Sea basin based on magnetic anomalies and age determined at site 768. In: Proc. Ocean Drill. Program, Sci. Res, pp. 343–393.
Roest, W.R., Verhoef, J., Pilkington, M., 1992. Magnetic interpretation using the 3-D analytic signal. Geophysics 57, 116–125.
Ross, H.E., Blakely, R.J., Zoback, M.D., 2006. Testing the use of aeromagnetic data for the determination of Curie depth in California. Geophysics 71, L51–L59.
Sajona, F., Maury, R., Bellon, H., Cotten, J., Defant, M., 1996. High field strength element enrichment of Pliocene-Pleistocene island arc basalts, Zamboanga Peninsula, Western Mindanao (Philippines). J. Petrol. 37, 693–726.
Salem, A., Ravat, D., Gamey, T.J., Ushijima, K., 2002. Analytic signal approach and its applicability in environmental magnetic investigations. J. Appl. Geophys. 49, 231–244.
Sales, A.O., Jacobsen, E.C., Morado Jr., A.A., Benavidez, J.J., Navarro, F., Lim, A.E., 1997. The petroleum potential of deep-water northwest Palawan Block GSEC 66. J. Asian Earth Sci. 15, 217–240.
Sandwell, D.T., Smith, W.H., 2009. Global marine gravity from retracked Geosat and ERS-1 altimetry: Ridge segmentation versus spreading rate. J. Geophys. Res. 114, B01411. http://dx.doi.org/10.1029/2008JB006008.
Sarewitz, D., Karig, D., 1986. Stratigraphic framework of western Mindoro Island, Philippines. Philipp. Geol. 40, 3–50.
Schlüter, H., Hinz, K., Block, M., 1996. Tectono-stratigraphic terranes and detachment faulting of the South China Sea and Sulu Sea. Mar. Geol. 130, 39–78.
Shi, H., Li, C.-F., 2012. Mesozoic and early Cenozoic tectonic convergence-to-rifting transition prior to opening of the South China Sea. Int. Geol. Rev. 54, 1801–1828.
Shin, Y.H., Choi, K.S., Xu, H., 2006. Three-dimensional forward and inverse models for gravity fields based on the Fast Fourier Transform. Comput. Geosci. 32, 727–738.
Silver, E.A., Rangin, C., 1991. Development of the Celebes Basin in the context of western Pacific marginal basin history. In: Proceedings of the Ocean Drilling Program, Scientific Results, pp. 39–49.
Sun, L., Sun, Z., Zhou, D., Liu, H., 2008. Stratigraphic and structural characteristics of Lile Basin in Nansha area. Geotecton. Metallog. 32, 151–158 (in Chinese).
Suzuki, S., Asiedu, D., Takemura, S., Yumul Jr., G., David Jr., S., Asiedu, D., 2000a. Composition of sandstones from the Cretaceous to Eocene successions in Central Palawan, Philippines. J. Geol. Soc. Philipp. 56, 31–42.
Suzuki, S., Takemura, S., Yumul, G.P., David, S.D., Asiedu, D.K., 2000b. Composition and provenance of the Upper Cretaceous to Eocene sandstones in Central Palawan, Philippines: constraints on the tectonic development of Palawan. Isl. Arc 9, 611–626.
Tamayo, R.A., Yumul, G.P., Maury, R.C., Polvé, M., Cotten, J., Bohn, M., 2001. Petrochemical investigation of the Antique Ophiolite (Philippines): Implications on volcanogenic massive sulfide and podiform chromitite deposits. Resour. Geol. 51, 145–164.
Tanaka, A., Okubo, Y., Matsubayashi, O., 1999. Curie point depth based on spectrum analysis of the magnetic anomaly data in East and Southeast Asia. Tectonophysics 306, 461–470.
Taylor, B., Hayes, D.E., 1980. The tectonic evolution of the South China Sea. In: Hayes, D.E. (Ed.), The Tectonic and Geologic Evolution of South Eastern Asian Seas and Islands, I, Am Geophys Union, Geophys Monogr, Washington, D.C., 23, pp. 89–104.
Taylor, B., Hayes, D.E., 1983. Origin and history of the South China Sea basin. In: Hayes, D.E. (Ed.), The Tectonic and Geologic Evolution of South Eastern Asian Seas and Islands, II, Am Geophys Union, Geophys Monogr, Washington, D.C., 27, pp. 23–56.
Weissel, J.K., 1980. Evidence for Eocene oceanic crust in the Celebes Basin. Geophys. Monogr. Ser. 23, 37–47.
Wessel, P., Smith, W.H., 1995. New version of the generic mapping tools. Eos Trans. AGU 76, 329.
Williams, H.H., 1997. Play concepts-northwest Palawan, Philippines. J. Asian Earth Sci. 15, 251–273.
Woodside, J., Carl, B., 1970. Gravity anomalies and inferred crustal structure in the eastern Mediterranean Sea. Geol. Soc. Am. Bull. 81, 1107–1122.
Xia, K., Huang, C., 2000. The discovery of Meso-Tethys sedimentary basins in the South China Sea and their oil and gas perspective. Earth Sci. Front. (China University of Geosciences, Beijing) 7, 227–238 (in Chinese).
Yao, Y., Liu, H., Yang, C., Han, B., Tian, J., Yin, Z., Gong, J., Xu, Q., 2012. Characteristics and evolution of Cenozoic sediments in the Liyue Basin, SE South China Sea. J. Asian Earth Sci. 60, 114–129.
Yumul Jr., G.P., Dimalanta, C.B., Marquez, E.J., Queaño, K.L., 2009. Onland signatures of the Palawan microcontinental block and Philippine mobile belt collision and crustal growth process: a review. J. Asian Earth Sci. 34, 610–623.
Zamoras, L.R., Montes, M.G.A., Queaño, K.L., Marquez, E.J., Dimalanta, C.B., Gabo, J.A.S., Yumul, G.P., 2008. Buruanga peninsula and Antique Range: two contrasting terranes in Northwest Panay, Philippines featuring an arc–continent collision zone. Isl. Arc 17, 443–457.
Zhang, S.-W., Li, C.-F., 2011. Magmatic activities in eastern China and adjacent seas revealed by 3D analytical signals of magnetic data. Geophys. Geochem. Explor. 35, 290–297 (in Chinese).